Int. J. Bio-Inorg. Hybr. Nanomater., 6(3): 113-129, Autumn 2017

Synthesis and characterization of optically active polyester thin-film bionanocomposite membrane achieved by functionalized cellulose /silica for gas permeation

H. Ahmadizadegan*, M. Ranjbar

Department of Chemistry, Islamic Azad University, Darab Branch, Darab, Iran

Received: 8 May 2017; Accepted: 11 July 2017

ABSTRACT: Optically active bionanocomposite membranes composed of polyester(PE) and cellulose /silica bionanocomposite (BNCs) are a novel method to enhance gas separation performance. Commercially available silica nanoparticles were modified with biodegradable nanocellulose through ultrasonic irradiation technique. Transmission electron microscopy (TEM) analyses showed that the cellulose/silica composites were well dispersed in the polymer matrix on a nanometer scale.The tensile stress–strain of the hybrids was investigated, and the resulting nanocomposites showed good mechanical properties.Thermo gravimetric analysis (TGA) data indicated an increase thermal stability of the PE/BNCs in comparison with the pure polymer. The permeability and selectivity of the PE/BNCs membranes as a function of the BNCs weight percentage were studied and the results obtained from gas permeation experiments showed that adding BNCs to the PE membrane structure increased the permeability of the membranes. Increasing the cellulose/silica mass fraction in the membrane increased the diffusion coefficients of gases considered in the current study. Further, antimicrobial test against pathogenic bacteria was carried out.

Keywords: *Antimicrobial; Bionanocomposite; Cellulose; Gas permeation; Optically active; Silica*

INTRODUCTION

In order to reduce the environmental pollution caused by polymers, attempts are being made to modify their structures by blending or combining them with other biodegradable materials (Albertson and Ljungquist, 1998, Tudorachi, *et al.*, 2000). Hence, the combination of polymers with cellulosic materials as, for example, blends, composites, nanocomposites and so on, are important areas of current research. There are very few reports of PE/cellulose/silica nanocomposite formation by polymerization technique. The production of BNCs has gained increasing attention in recent years. Cellulose, one of the world's most abundant, natural and renewable biopolymer resources, is widely present in various forms of bio-mass, such as plants. In cellulosic plant fibers, cellulose is present in an amorphous form, but is associated with crystalline phases through both intermolecular and intramolecular hydrogen bonding in which cellulose does not melt before thermal degradation (Klemm, *et al.*, 2005). Cellulose is organized

(*) Corresponding Author-e-mail: h.ahmadizadegan.2005@gmail.com

in fibrils, which are aligned parallel to each other, surrounded by a matrix of lignin and hemicellulose. The properties of cellulose including mechanical state, low density and biodegradability (Zimmerman, *et al.*, 2005) depend on the type of cellulose which is present. Owing to the abundance of hydroxyl groups existent on the surface of cellulose nanocrystals, reactive BNCs can be modified with different chemical groups to accomplish the expected surface modification like esterification and silylation or polymer grafting, which could successfully functionalize BNCs and facilitate its dispersion into different polymer matrices (Habibi, *et al.*, 2010). Therefore, BNCs is considered as one of the ideal nano-reinforcing agents for polymer matrices (including water soluble and water-insoluble polymer systems) and has been used into many polymer matrices to produce reinforced nanocomposites (Cao, *et al.*, 2011). In addition, low density, low energy consumption, inherent renewability, biodegradability and bio- compatibility are also good advantages of environmentally-friendly BNCs (Siro and Plackett, 2010). Because of good dispersion of BNCs in water (Liang, *et al.*, 2007), fabrication and application of hydrogels including NCC without modification have many advantages versus other nanofillers such as polymer and metal nanoparticles. The improved interface between nanofillers and polymer matrix is beneficial to the properties of polymer-based nanocomposites. In nanocomposites, hydrogen bonding between BNCs and polymer matrix plays an important role in determining polymer- BNCs interaction (Wu, *et al.*, 2009). Cellulose is the primary component providing strength to wood and other plant structures. Recently, cellulose based smart material has received much attention due to its unique material nature for possible sensors, actuators, and electronic applications (Zheng, *et al.*, 2013, Moon, *et al.*, 2011, Tobjork and Osterbacka, 2011). Similarly, silicon has been paid much attention of potential flexible electronics as an abundant semiconductor material for polymer functionality based reaction process (Nyholm, *et al.*, 2011, Song, *et al.*, 2017). For this reason, there are number of studies on synthesis of the cellulose-polymer composites to enhance the material performances such as thermal, mechanical, electrical, and morphological properties of the polymers (Athawale and Lele, 1998, Chang, *et al.*, 2003). Generally, the composite processes with metal oxide based materials are widely used in material design, fabrication, and applications in recent nanotechnologies. It is reported that nanofibers and nanoporous materials have been used to obtain relatively large surface, unusual strength, high surface energy, and high surface activity compared to its volume ratio of existing material properties. The cellulose molecular and nanosilicon dioxide particles with organic groups need to be further modified by sol-gel crosslinking process. Moreover, the new hybrid material of silica-cellulose with uniform sized, shape and composition has a feasibility to be used in wide applications such as catalysis and photonics. Also, the immobilization of certain strains of bacteria to withstand the effects of number of common antibiotics has led us to find novel strategies for the treatment of infections associated to antimicrobial properties and biomaterials (Hou, *et al.*, 2008, Innocenzi and Lebeau, 2005, Laine, *et al.*, 2001, Von Nussbaum, *et al.*, 2006, Tamaki, *et al.*, 2001). The preparation of hybrid organic–inorganic composites has been developed and studied during the last decade, because hybrids show controllable chemical and physical properties by combining the effects of organic polymers and inorganic compounds (Tyan, *et al.*, 1999, Abdalla, *et al.*, 2002, Zhang, *et al.*, 2005, Ahmad and Mark, 2001, Dinari and Ahmadizadegan, 2015, Ahmadizadegan, 2016). Membrane-based gas separation processes have become more attractive over traditional technologies in different gas separation and purification processes, such natural gas treating, air separation, olefin/paraffin separation, and hydrogen purification. They offer lower capital and operating costs, lower energy requirements, and ease of operation (Yu, *et al.*, 2014). The gas separation performance of many polymers has been studied in the literature (Wu, *et al.*, 2016). One of the most important and practical methods for improving the gas separation performance of polymeric membranes is the incorporation of inorganic materials like silica nanoparticles into the polymer matrix. The presence of nanoparticles in the polymer matrix leads to the enhancement of the mechanical strength and thermal stability of the polymer as well as increasing the permeability of nanocomposite membranes (Kim and Lee, 2001).

Therefore, the present study is focused on synthesis of optically active bionanocompositeme mbranes. Cellulose/silicais used for enhancing strength and thermal resistance of membranes. It also exhibits good affinity for some gas molecules and can be used as potential silica in nanocomposite gas separation membrane preparation. Cellulose/silica, having hydroxyl groups containing surfactant can act as pseudo cross-linker. Nanocomposite membranes were fabricated by the solution casting method with different loadings of cellulose/silica. Cellulose/silica dispersion and morphology of the prepared nanocomposite were characterized using field emission-scanning electron microscopy (FE-SEM), and transmission electron microscopy (TEM) techniques. Characteristics of membranes such as thermal degradation and glass transition temperature (T_g) were evaluated by TGA and DSC. Gas permeation properties of CO_2, CH_4, N_2, and O_2 are reported as a function of particle concentration. Further, antimicrobial test against pathogenic bacteria was carried out.

EXPERIMENTAL

Equipment's

Fourier-transform infrared (FT-IR) spectra were measured on a Nicolet Impact 410 FT-IR spectrometer. Proton nuclear magnetic resonance (^{1}HNMR) experiments were carried out on a Bruker 510 spectrometer using deuterated dimethyl sulfoxide as a solvent. Differential scanning calorimeter (DSC) measurements were performed on a Mettler Toledo DSC821e instrument at a heating rate of 20°Cmin^{-1} from 80°C to 300°C under nitrogen. Thermo gravimetric analysis (TGA) on a PerkinElmerPyris-1 thermal analyzer system was employed to evaluate the thermal stability of the polymers. To remove water, the membranes were dried and kept in the TGA furnace at 150°C under a nitrogen atmosphere for 15min before testing. The samples were evaluated in the range of 100°C–800°C at a heating rate of 10°Cmin^{-1} under nitrogen atmosphere. Mechanical properties of the membranes were evaluated at room temperature on SHIMADZU AG-I 1KN at a strain rate of 2 mm min1, and a 500 N load cell was used. The samples were prepared by cutting the membranes in dumbbell shapes of 15 mm × 4 mm. At least three measurements for each membrane were taken and the average value calculated. The gas permeability of the polymer membranes with thickness around 30 mm was measured with an automated Diffusion Permeameter (DP-100-A) manufactured by Porous Materials Inc., USA, which consists of upstream and downstream parts separated by a membrane. Gases measured include N_2, O_2, CH_4 and CO_2. The permeation cell was placed in a thermostatically controlled housing for maintaining isothermal measurement conditions. The reproducibility of the measurements was checked from three independent measurements using the same membrane, and it was better than ±5%.

Materials

3,5-bis(trifluoromethyl)phenol, 1-chloro-4-nitrobenzene, L(-)-tartaric acid, and tetrahydrofuran (THF) were obtained from Guoyao Chemical Plant (Shanghai, China). N, N-Dimethyl-formamide (DMF) was provided by Shanghai Gaoqiao Petrochemical Co. (Shanghai, China). Nanopowder silica was obtained from Neutrino (Tehran, Iran) with an average particle size of 10–15 nm and 99.99%purity. Nitrogen, methane, oxygen and carbon dioxide gases from BOC were used for the permeation study. The cellulose nanofibers (CNFs) used in this study was provided by the Institute of Tropical Forestry and Forest Products (INTROP), Malaysia, and was isolated from the kenafbast fibers (Hibiscus cannabinus). The details of the CNFs isolation process are reported elsewhere (Jonoobi*et al.*, 2009). The selected fungus was a white rot fungus (Trametes versicolor), which was obtained from the National Collection of Biology Laboratory, University of Tehran, Iran. Glycerol, methanol, acetone, and acetic anhydride (95%), pyridine, and malt extract agar (MEA) were purchased from the Merck Chemical Co., Germany. All the materials and solvents that were used were obtained from the suppliers without further purification.

Synthesis of chiral1-(4-(3,5-bis(trifluoromethyl)phenoxy) phenyl)-3,4 dihydroxypyrrolidine-2,5-dione monomer

In a 50 ml three-neck round-bottomed flask equipped with a stirring bar under nitrogen atmosphere, 1.00 g (6.13 mmol) of 3,5-bis(trifluoromethyl)phenol, 0.99 g

(6.13 mmol) of 1-chloro-4-nitrobenzene, (6.13 mmol) of potassium carbonate, and 20 mL of DMAc was added. The solution was stirred at 125°C for 4 h. After cooling to room temperature, the mixture was poured into 300 mL of methanol. The precipitate was dried at 55°C under vacuum and the product was recrystallized from glacial acetic acid to obtain the nitro monomer in 79% yield. In the second step, a mixture of hydrazine monohydrate (3 mL), nitro compound (2.00 g, 7.06 mmol), a catalytic amount of 10% Pd/C (0.15 g), and ethanol (90 mL) was heated at reflux for 14 h. To remove Pd/C, the reaction solution was filtered and purified by recrystallization from methanol and then it was dried in vacuum (80% yields).

4-(3,5-bis(trifluoromethyl)phenoxy)benzenamine and the chiral reagent L (-)-tartaric acid were added to DMF under magnetic stirring, and the reaction mixture was heated to 55°C and refluxed for 24 h. After the reaction was completed, the solution containing dihydroxyl groups and the trifluoromethyl group was obtained. For $C_{18}H_{11}F_6NO_5$ monomer the yield is 60–65%. Rotation value ($[\alpha]^{25}_D$) of monomer chiral diol in concentration 4×10^{-2} mg/mL (DMF) is -35.3 (Scheme 1).

FT-IR (KBr, cm^{-1}): 3455(s), 3443 (s), 3118 (w), 3065 (w), 1725 (s), 1623 (s) 1560 (m), 1556 (m), 1312 (w), 1125 (w), 850 (m), 645 (w).

^{1}HNMR (500 MHz, DMSO-d_6, ppm): 3.54 (s, 2H, OH), 4.54 (d, 2H, C-H), 6.86-6.88 (d, 2H, Ar-H, J= 3.6 Hz), 7.10-7.13 (d, 2H, Ar-H, J= 4.4), 7.23 (s, 1H, Ar-H),7.55-7.57 (d, 2H, Ar-H, J= 3.6.0).

^{13}CNMR (125 MHz, DMSO-d_6), δ (ppm): 84.67 (C-O), 121.11 (Ar), 123.77 (Ar), 1256.98 (Ar), 128.19 (Ar), 131.26 (CF3), 132.29 (Ar), 133.17 (Ar), 137.22 (Ar), 167.17 (C=O).

Elemental analysis: Calcd. For $C_{18}H_{11}F_6NO_5$ (435.27 g mol^{-1}): C, 49.67%; H, 2.55%; N, 3.22%. Found: C, 50.61%; H, 2.53 %; N, 3.27%.

Polymer synthesis

A solution of Py (0.20 ml) with tosyl chloride (TsCl) (0.29 g; 1.55×10^{-3} mol) after 30 min stirring at room temperature, was treated with DMF (0.10 ml; 1.25×10^{-3} mol) for 30 min and the mixture was added dropwise to a solution of diacid (0.10 g; 4.63×10^{-4} mol) in Py (0.20 ml). The mixture was maintained

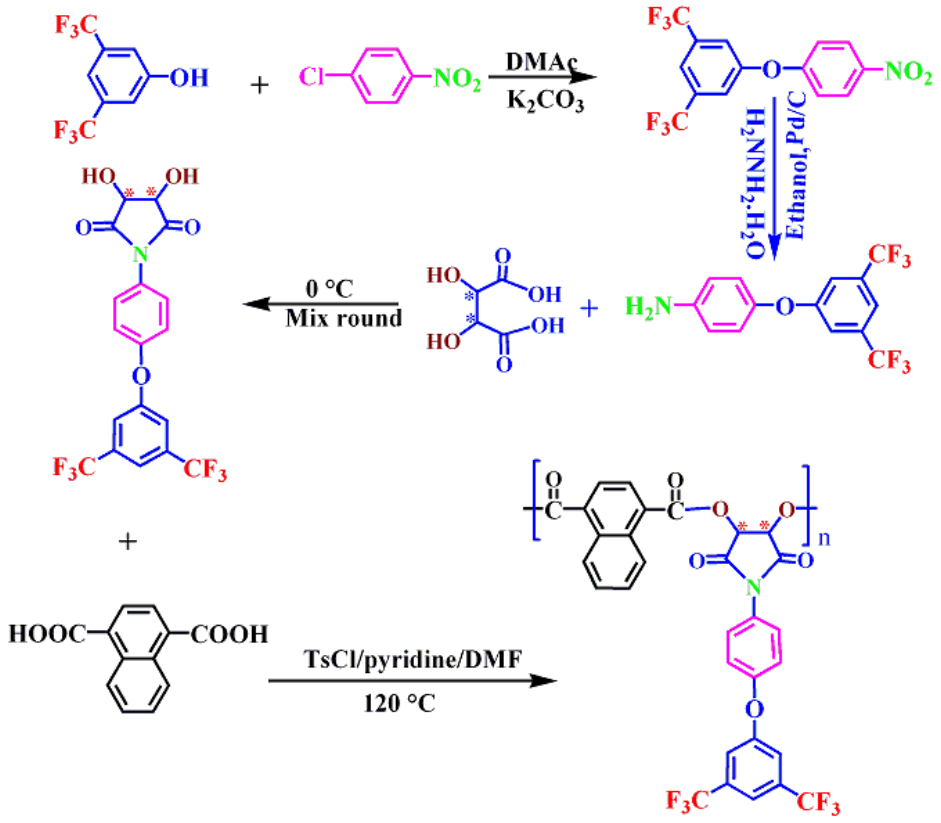

Scheme 1.Synthesis of chiral diol monomer and Synthesis of PE with a trifluoromethyl pendent group.

at room temperature for 30 min and then chiral 1-(4-(3,5-bis(trifluoromethyl)phenoxy)phenyl)-3,4 dihydroxypyrrolidine-2,5-dione (0.28 g; 4.73×10^{-4} mol) was added to this mixture and the whole solution was stirred at room temperature for 30 min and then at 120ºC for 4 h. As the reaction proceeded, the solution became viscous and then the viscous liquid was precipitated in 30 ml of methanol to give 1.24 g pale brown powder PE (95% yield) and the specific rotation was measured in concentration 4×10^{-2} mg/mL (DMF) ($[\alpha]^{25}_{D}$= -25.12). The Number average molar mass (M_n), Mass average molar mass (M_w) and Polydispersity index (M/M_n) of PE is 84255, 157225 and 1.87 respectively (Scheme 1).

FT-IR Peaks (KBr, cm^{-1}): 3435 (w, br), 3025 (w), 3010 (w), 1755 (s), 1727 (s), 1535 (m), 1352 (s), 1249 (w), 1221 (m), 1175 (m), 1173 (m), 1132 (w), 1055 (w), 733 (m).

^{1}HNMR (500 MHz, DMSO-d_6, ppm): 5.26 (d, 2H, C-H), 6.77-6.79 (d, 2H, Ar-H, J= 4.0 Hz), 6.93 (s, 1H, Ar-H), 7.21-7.23 (d, 2H, Ar-H, J= 4.0 Hz), 7.42-7.44 (d, 2H, Ar-H, J= 2.0), 7.57-7.59 (d, 2H, Ar-H, J= 4.0), 7.63-7.65 (d, 2H, Ar-H, J= 3.0), 7.74-7.77 (d, 2H, Ar-H, J= 4.6).

GPC measurements of resulting PE: M_n: 84255, M_w: 157225, PDI: 1.87.

Elemental analysis: Calc. For $C_{32}H_{21}F_6NO_7$ (645.12 g mol^{-1}): C, 59.54%; H, 3.28%; N, 2.17%. Found: C, 60.11%; H, 3.25 %; N, 2.19%.

Surface functionalization of silica nanoparticles with nanofiber cellulose(Ahmadizadegan, 2017)

Nanofiber cellulose was modified silica nanoparticle by ultrasonic irradiation. Typical steps were given as follows: nano silica was dried at 120°C in an oven for 24 h to remove the adsorbed water. 0.10 g of dried nano silica in DMF solution by a sonication treatment for 20 min (through an ultrasonic instrument MISONIX, 100 W), then 0.05 g of nanofiber cellulose was added to this mixture and sonicated for 45 min. The mixture was filtered and dried at 75°C for more than 24 h (Scheme 2).

Synthesis of PE/cellulose/silica nanocomposite membrane

Cellulose/silica (4, 8 and 12weight% with respect to PE) was suspended in DMAc and vigorously stirred at

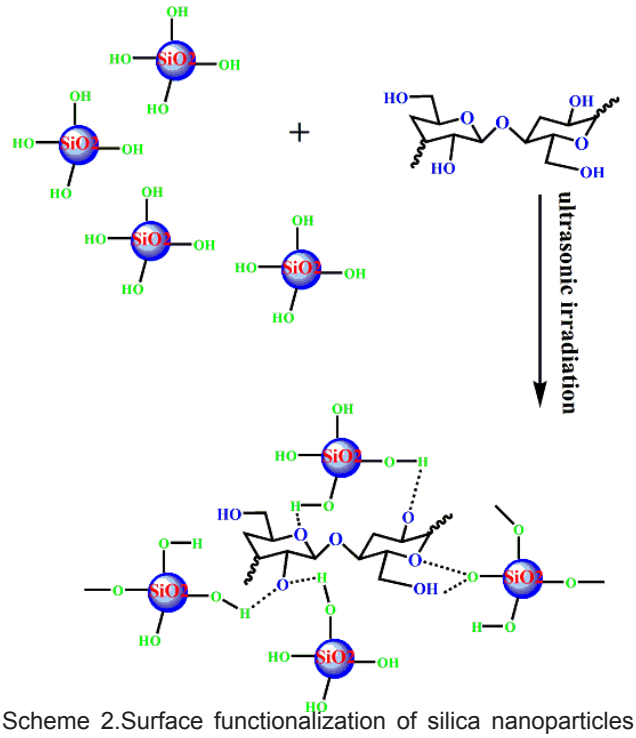

Scheme 2.Surface functionalization of silica nanoparticles with nanofiber cellulose

30°C for 24 h. 10% PE by weight was dissolved in the same solution at 60°C under stirring. The composite solution was then sonicated for 4 h and cast on a glass plate (Scheme 3). The film was then dried under ambient conditions for 2 days and then cured under vacuum at different temperatures. The sequence of heating was; 50°C for 2 h, 100°C for 2 h, 120°C for 2 h and 135°C for 24 h. Bionanocomposite membranes with 4, 8 and 12 weight% of cellulose/silica content nomenclature as PE/cellulose/silica 4%, PE /cellulose/silica 8% and PE/cellulose/silica 12%, respectively.

Gas Permeability Measurement

The pure gas (N_2, O_2, CH_4 and CO_2) transport properties of prepared membranes were determined using a constant volume/variable pressure method as described in detail by Panndey, *et al.* (Panndey, 2001). The feed side gas pressure was 10 bar (gauge) and the active area of the membrane cell was 13.1 cm^2. The specifications of the constant volume/variable pressure setup are also described in detail elsewhere (Sadeghi, *et al.*, 2009). The gas permeability of membrane was calculated using the following equation:

$$P = \frac{273.15V}{76p_0AT}\frac{dp(t)}{dt} \quad (1)$$

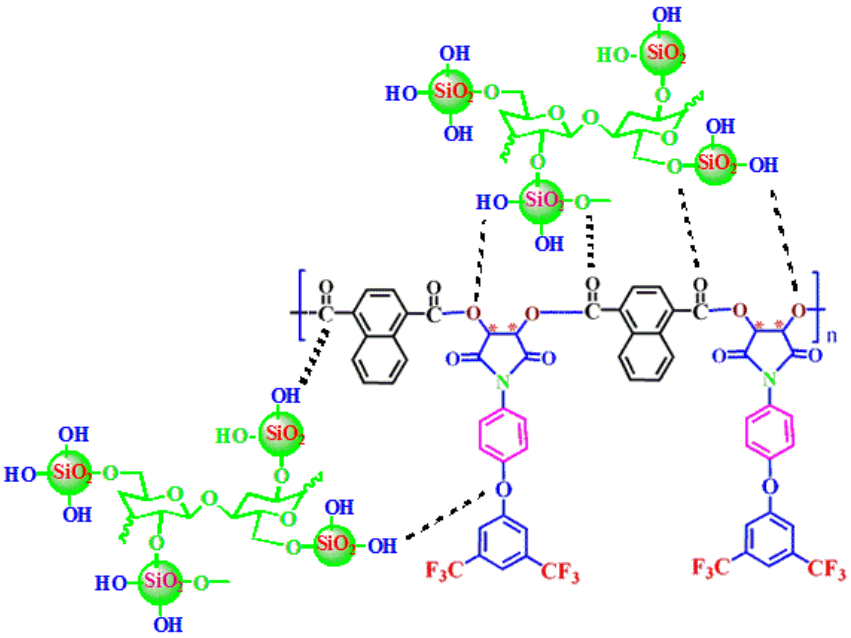

Scheme 3.Preparation of PE/cellulose/silica bionanocomposite

Where P is the permeability in barrer (1 barrer=1×10^{10} cm^3 (STP) cm/cm^2 s cmHg), V, the volume of the down-stream chamber (cm^3), A, the effective membrane area (cm^2), L, the membrane thickness (cm), T, the experimental temperature (K), dp(t)/dt, the steady rate of pressure measured by a pressure transducer in the down-stream chamber and p_0, the feed pressure with the same unit of p(t). The diffusion coefficient (D) was calculated by the time-lag method as below:

$$D = \frac{L^2}{6\theta} \quad (2)$$

Where θ is the time lag (s), the intercept obtained from extrapolating the linear region of the p(t) versus the time plot to the time axis D is the diffusion coefficient (cm^2/s).

The solubility coefficient (S) (cm^3 (STP)/cm^3 cmHg) was calculated as:

$$S = \frac{P}{D} \quad (3)$$

The ideal selectivity of membranes ($\alpha_{A/B}$) was determined from pure gas permeability as follow:

$$\alpha_{A/B} = \frac{P_A}{P_B} \quad (4)$$

Synthesis of PE/cellulose/silica Nanocomposites for Antimicrobial Test

The Agar Diffusion Test, The antimicrobial activity of PE/cellulose/silica nanocomposites was evaluated against B. cereus and E. coli. The amount of 0.2 mL of fresh cultures of organism was inoculated into 5 mL of sterile Luria Broth and incubated for 3–5 hrs. for the standard culture to Mc Farland standards (106 CFU/mL). The calculated amount of 100 µL of revived culture was added on agar medium and poured on two replicate plates having a diameter of about 8mm, 50 µL samples of PE/cellulose/silica nanocomposites were added, and 50 µL antibiotics (ampicillin) was also added in the separate standard. The Petri plates were incubated at 37°C for 20 and 24 hrs.Colony-Forming Unit,The amount of 100 µL of the serial dilution 107 of the culture with and without PE/cellulose/silica nanocomposites was inoculated on agar plate and was spread over it. The plates were incubated for 20–24 hrs. and observed for bacterial growth and viable count per 100 µL for a dilution occurred.

Antimicrobial Test of PE/cellulose/silica nanocomposites, The stock suspension of PE/cellulose/silica nanocomposites with concentrations of 1mg/mL was prepared by suspending them in ethanol solution and sonicated for 10 minutes to get the homogenous suspension, for the homogeneous light was kept in UV for 30min for sterilization. The overnight culture of

the Bacillus's Cereus (F481072) and E. coli (ATCC 35150) was added to Luria Broth with different concentration of cellulose/silica nanocomposites, respectively, and incubated at 37°C for 20 and 24 h to study the affected microbial activity of hybrid nanoparticles.

RESULTS AND DISCUSSION

Synthesis and characterization of chiral 1-(4-(3,5-bis(trifluoromethyl)phenoxy)phenyl)-3,4 dihydroxypyrrolidine-2,5-dione monomer

The chemical structure of the synthesized chiral diol was confirmed by elemental analyses (reported in the experimental section), FT-IR, ^{1}HNMR and 13CNMR spectroscopy techniques.In the 1HNMR spectrum of the chiral diol, the aromatic protons appeared in the range of 6.86–7.55 ppm, and the hydroxyl groups appeared at 3.54 ppm. Moreover, the chiral hydrogen's were observed at 4.54 ppm (Fig. 1). In the spectrum of chiral diol (Fig. 1a), Fig. 1b shows the ^{13}CNMR spectrum of chiral diol. The aromatic carbons are presented in the range of 121.11–167.17 ppm and the carbon of chiral is appeared at around 84.67 ppm (Fig. 1b).

Characterization of the optically active polyester

The chiral PE was prepared by the one/pot, high/temperature solution polymerization of diacid monomer with aromatic chiral1-(4-(3,5-bis(trifluoromethyl) phenoxy)phenyl)-3,4-dihydroxypyrrolidine-2,5-dione at 120°C. The resulting PE showed inherent viscosity 1.24 dL g^{-1} at a concentration of 0.5 g dL^{-1}. Moreover, the number average molecular weight (M_n), weight average molar weight (M_w) and polydispersity index (PDI) (reported in the experimental section) of the synthesized polymer were further supported by GPC measurements. The FT-IR spectra of the PE showed the characteristic absorption bands of the (C=O ester and imide absorption at 1755, 1727 cm^{-1} and 1352 (C–N stretching) and 733 cm^{-1} (C=O bending). Fig. 2 exhibits a typical 1HNMR spectrum of the PE, in which all the peaks have been readily assigned to the

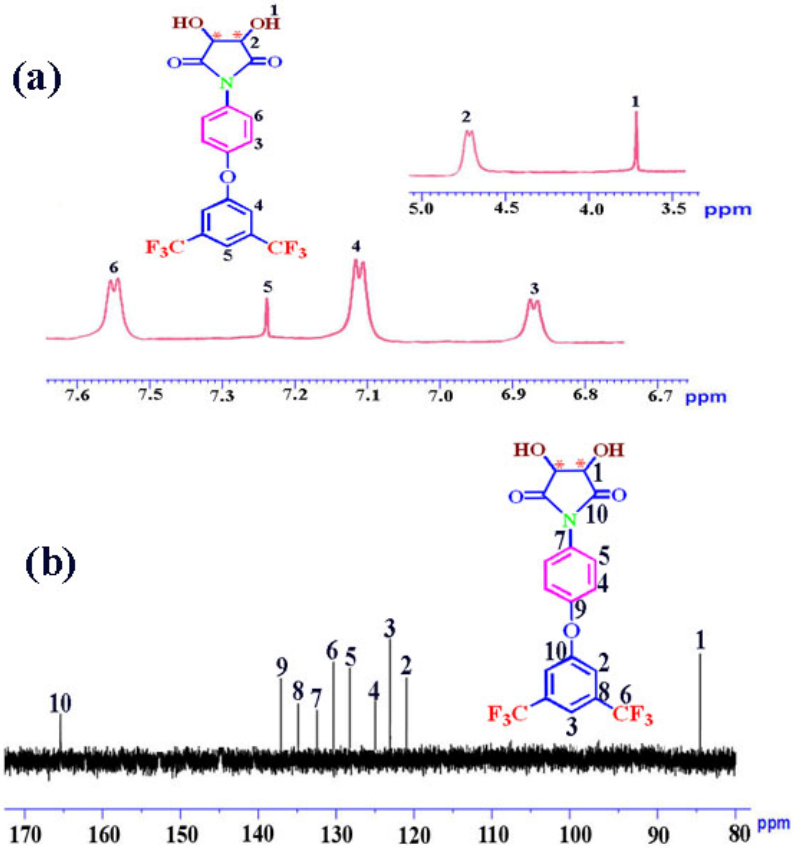

Fig. 1. ^{1}HNMR (500 MHz) spectrum of chiral diol monomer in DMSO-d_6 at R.T and ^{13}CNMR (125 MHz) spectrum of chiral diol monomer in DMSO-d_6 at R.T

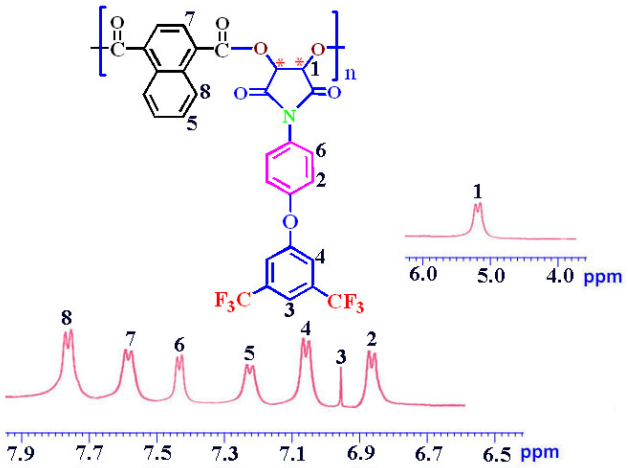

Fig. 2. ^{1}HNMR (500 MHz) spectrum of PE in DMSO-d_6 at RT

hydrogen atoms of the repeating unit and no hydroxyl or acid protons at 10–12 ppm appears, indicating that complete polymerization of PE. Moreover, the peaks at around 3.54 ppm corresponding to the hydroxyl groups in the ^{1}HNMR spectrum of diol disappeared completely in the ^{1}HNMR spectrum of the polymer (Fig. 2). The PE was also characterized by elemental analysis techniques, and the results are in good agreement with the calculated ones for the proposed structures (reported in the experimental section). These results in sum confirmed the successful formation of the new chiral PE.

FT-IR spectroscopy of PE/cellulose/silica nanocomposites membrane

FT-IR studies were carried out to confirm the identification and bond structure of associated functional groups of as-synthesized silica impregnated cellulose using optimized parameters. The infrared absorption spectra of cellulose, silica NPs and cellulose/silica nanocomposites were observed in the 4000-400 cm^{-1} wave-number range (Fig. 3). Comparison of citrus cellulose and silica NPs with cellulose/silica composite demonstrates an appropriate coincidence. The intermolecular hydrogen bonds in cellulose may be weaker than those in the cellulose/silica and the low crystallinity and intermolecular hydrogen bonds in cellulose make it more reactive component when participating in a chemical reaction.

The FT-IR spectrum of Silica (Fig. 3a) show main absorption bands at 3400, 1560, and 1365 cm^{-1}, which

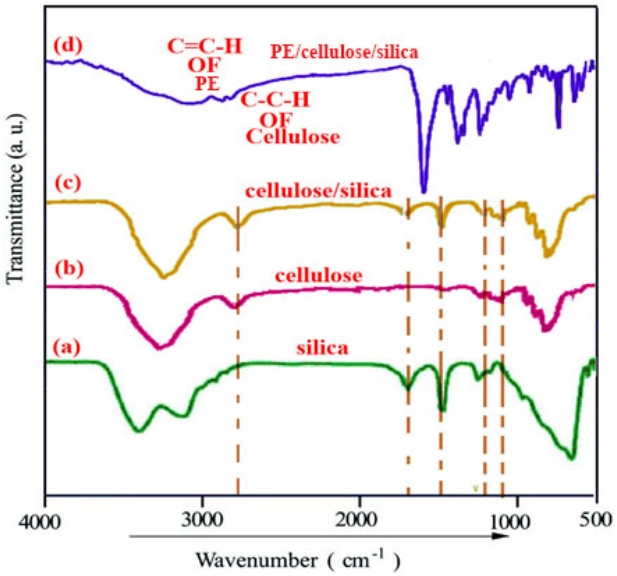

Fig.3.(a) FT-IR spectra of pure silica nanoparticle, (b) pure cellulose, (c) modified silica nanoparticle and (d) PE/cellulose/silica (12%)

correspond to the O–H mode, and peak at 450 cm^{-1} is the characteristic absorption of Si–O bond. In the cellulose spectrum (Fig. 3b), the stretching and bending modes of theOH group were viewed at 3455 and 1525 cm-1,respectively.The peak at 1030 cm^{-1} originates from the C–O stretching of cellulose. Such results and appeared new bands at 2855 cm^{-1} in the FT-IR spectrum of modified Silica nanoparticles indicate that the cellulose have been successfully grafted onto the surface of Silica nanoparticles (Fig. 3c).The incorporation cellulose/silica in PE caused the slight changes in the intensities of absorption bands to 1625 and 1575 cm^{-1} as well as the formation of new absorption bands in the range of 400–700 cm^{-1}. Peak around 400–700 cm^{-1} is attributed to the Si-O stretching of Silica. This corroborated the presence of Silica nanoparticles present in the PE matrix (Fig. 3d).

XRD analysis of the PE/cellulose/silica nanocomposite films

XRD analyses were conducted to investigate the crystalline properties of cellulose, the synthesis of cellulose/Silica nanocomposites and the micro-structural changes in the cellulose sheets caused by the Silica nanoparticles. Fig.4 shows the XRD patterns of the pure cellulose (a), pure Silica (b) and cellulose/Silica (c). The characteristic peaks of cellulose ap-

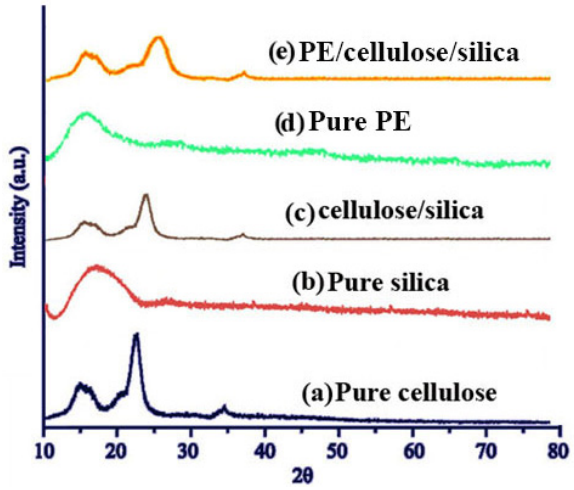

Fig.4. (a) XRD spectra of pure cellulose, (b) pure silica nanoparticle, (c) modified silica nanoparticle, (d) pure PE and (e) PE/cellulose/silica (12%)

peared at 2θ values of 23.1° and 34.9° corresponds to the structure of planes particles. Neither a new peak nor a peak shift compared with the pure cellulose indicates that the cellulose/Silica nanocomposite films consist of two phase structures that may be polymer and nanoparticles. These observations show that the addition of the cellulose/Silica causes an overall increase in crystallinity of pure PI that can be effective on the final proprieties of biocomposites films. Fig. 4 displays the X-ray diffraction (XRD) patterns ofcellulose/Silica (c), pure PE (d) and PE/cellulose/Silica (12%) (e). The average particle size of nanoparticles was estimated based on Scherrer correlation of particle diameter (D) $D=K\lambda/\beta\cos\theta$ where K is the Scherrer constant, λ the X-ray wavelength, β the peak width at half-maximum, and θ is the Bragg diffraction angle. The average size of the Silica calculated from the width of the diffraction peak according to the Scherrer equation is approximately less 30 nm. This is in agreement with the size of used Silica nanoparticles. Pure PE and pure silica (Fig. 4b) were totally amorphous in nature, which did not show any sharp diffraction peaks.

FE-SEM and TEM study of PE/cellulose/silica nanocomposite films

Fig. 5(a-d) shows the FE-SEM micrographs of PE/cellulose/silica (12 wt%). The average particle size of the nanoparticles was in the range of 25-30 nm. The FE-SEM images of PE/cellulose/silica (12 wt%) reveal that the cellulose/Silica BNCs were homogeneously dispersed in the polymer matrix. Due to treating Silica filler with modifying agents such as cellulose and ultrasound irradiation that effect on the distribution and particle size of the nanoparticles the compatibility of Silica filler with PE matrix are able to be improved. TEM has confirmed to be a powerful tool for studying the dispersion of nanocomposits embedded within a polymer matrix. The TEM micrograph of the PE/cellulose/silica (12 wt%) in Fig. 6 (a-c) shows that silica nanoparticle were homogeneously dispersed in polymer matrix. The modified cellulose/silica might

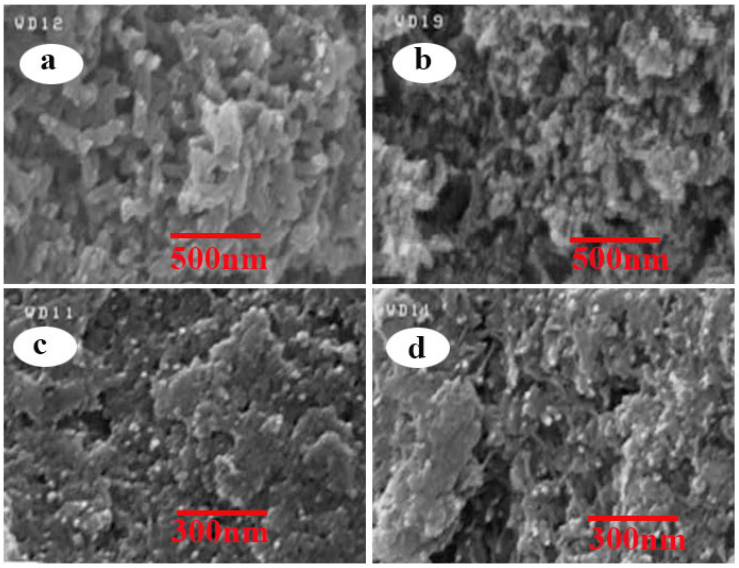

Fig.5.FE-SEM (a-c) micrograph PE/cellulose/silica (12%)

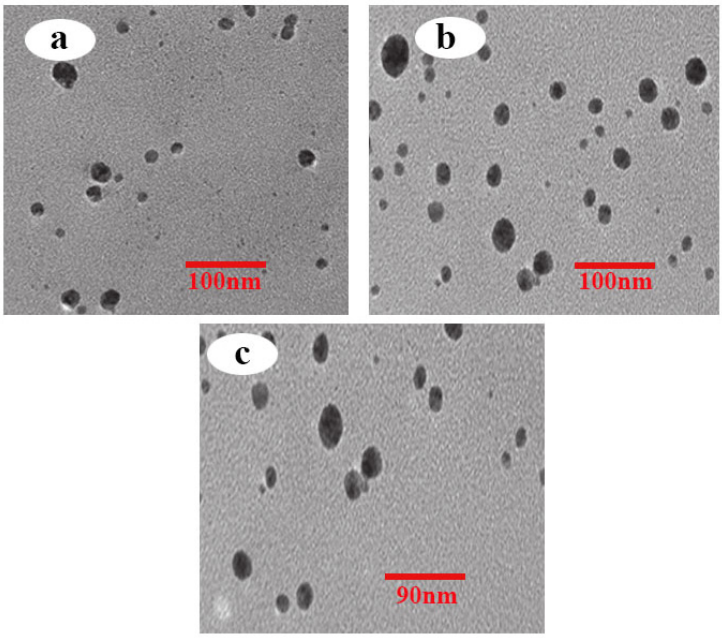

Fig.6. TEM micrographs of PE/cellulose/silica (12%) bionanocomposite membranes

be dispersed absolutely and will combine with PE via the H-bonding of O-H coupling agent with –O-, N, C=O groups in PE. In addition –OH groups on the surface of Silica nanoparticle can bond to the N and O group of PE through interchange hydrogen bonding. The average size of the nanoscale Silica particles is about 25 nm. The obtained results show that the surface modification plays a main role in dispersion of Silica nanoparticles.

Thermal properties of nanocomposite films

The thermal stability of PE/cellulose/silica NCs and pure PE as references was investigated at the heating rate of 20°C min^{-1} from 20 to 800°C. Fig. 6 shows TGA curves for the four samples pure PE, PE/cellulose/silica NC4%, PE/cellulose/silica NC8% and PE/cellulose/silica NC12%. The pure PE film is quite stable up to 465°C. The weight of the pure PE film remained around 98% under 505°C, and then substantially decreased from 525°C to 600°C (Fig. 7). The PE/cellulose/silica NC film showed a similar pattern of weight loss but at higher temperature (over 500°C) than the pure PE films and the decomposition was completed at around 600°C. The decomposition temperature at 5% (T_5%) weight loss for these composites increases with the cellulose/silica nanofillers loading. About 70°C improvements in T_5% is found in 12 wt% cellulose/silica nanofillers loading. Excellent thermal stability should be attributed to the contribution of the existed covalent bonding interaction between PE and cellulose/silica nanofillers. The 10% weight loss temperatures (T_{10}%) of the PE is 540°C and for NC materials with 4, 8 and 12 wt% of cellulose/silica nanofillers, it is 560, 575 and 580°C, respectively. The char yields at 800°C of the NCs with different cellulose/silica content are higher than that of pure PE which provided more evidence of completely organic inorganic bonding. The char yield of NCs was from 52 to 65% at 800°C. By comparison of the thermal properties of these hybrid materials with different NCs with

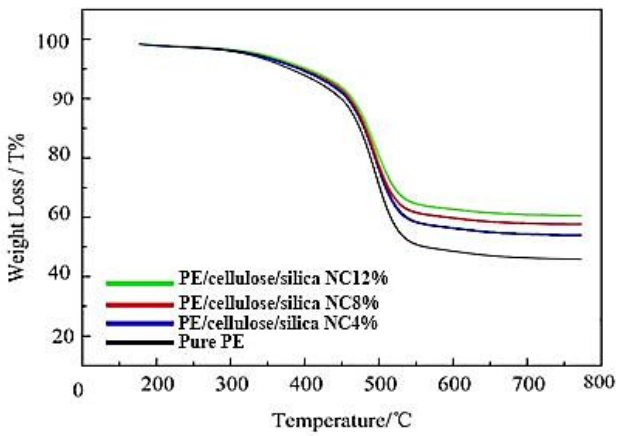

Fig. 7.TGA thermograms of PE and PE/cellulose/silica with different cellulose/silica content

similar structures the results show that these hybrids had higher thermal stability because of the good interaction between PE and cellulose/silica NCs. Hence, incorporation of the PEwith cellulose/silica due to the strong covalent and partial hydrogen bonding networks formed during the process and the thermal properties was enhanced.

Mechanical properties of nanocomposites films

The effects of cellulose/silica NCs loading on the tensile properties of PE/cellulose/silica films were investigated and the results are presented in Fig. 8. Filler consisting entirely of cellulose/silica generally increases the ultimate strength, but decreases the maximum extensibility. The mechanical properties of NCs largely depend on the external load transfer between the reinforcing nanofiller phase and the matrix (Qian,*et al.*, 2000). According to the previous study (Ahmadizadegan, 2016), the strength should be reduced if there are no bonding sites between the organic polymer phase and the inorganic TiO_2 phase due to the inert nature of the PIs and the weak interactions between these polymers and the TiO_2. In this case, the cellulose/silica acts as nonreactive and non-reinforcing filler. It is generally believed that external stress on a polymer composite is transferred from the continuous phase (polymer matrix) to the discontinuous phase (filler). Therefore, the ultimate properties of the NCs are dependent on the extent of bonding between the two phases, the surface area of the cellulose/silica, and the arrangements between the silica particles. As can be seen in Fig. 8, the tensile strength of PE/cellulose/silica NCs films is significantly increased compared with the pure PE. The maximum stress at break (ultimate strength) was found to increase initially with increase in cellulose/silica content, and at 8 wt% cellulose/silica showed a maximum value of 114.55 MPa (relative to the 97.12 MPa of the neat PI) representing considerable improvement in tensile strength. As the cellulose/silica content increases (12 wt%), the tensile strength of PE/cellulose/silica films decreases, but still better than the pure PE film because of increasing brittleness. According to the Fig. 8, ultimate strength and initial modulus were increased with cellulose/silica contents, but ultimate elongation decreased with the increase of cellulose/silica contents, especially at higher cellulose/silica content. For elongation at break, the sample geometry (most importantly the film thickness) is an additional factor to consider and may be the determine factor why the 8% wt% cellulose/silica sample shows the best result. The above results showed that the interactions between the PE and the cellulose/silica are very important.

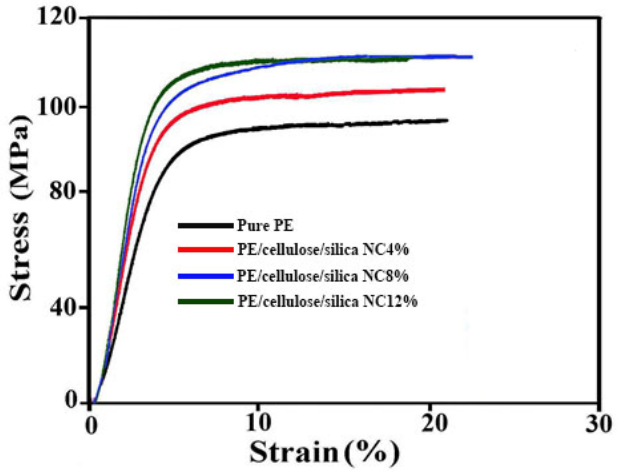

Fig. 8. Mechanical properties for pure PE with various cellulose/SiO_2 compositions

Gas permeation properties of PE/cellulose/silica nanocomposite membranes

Permeability and selectivity of pure gases through the membranes

The permeability of pure nitrogen, oxygen, methane and carbon dioxide gases was measured on the pure polymer and nanocomposite membranes of PE/cellulose/silica at 10 barg and 25°C. The results are given in Fig. 9 shows that the order of permeability of gases in both pure and composite membranes is as follows:

$$P_{CH4}<P_{N2}<P_{O2}<P_{CO2}$$

As known, permeation of molecules through polymeric membranes occurs via solution-diffusion mechanism. Considering that PE polymer is a conductive polymer, the process of gas separation on this polymer is performed based on domination of diffusion mechanism which can be described as molecular sieving. Table 1 reveals the investigations on the kinetic diameter of the relevant gases that the kinetic diameter of studied gases changes as follows:

$$d_{CO2}<d_{O2}<d_{N2}<d_{CH4}$$

Table 1. The kinetic diameter and condensability of the relevant gases

Kinetic diameter (Å)	Condensability temperature (K)	Gas
3.30	195	CO_2
3.80	149	CH_4
3.46	107	O_2
3.64	71	N_2

The order of permeability of gases is exactly contrary to the kinetic diameters of studied gases. So, it was found that diffusion is the dominant mechanism in permeability of gases through the PE and PE/cellulose/silica membranes, and the gases with smaller molecular size have the higher permeability in the membranes.As shown in Fig. 8, the permeability of gases increased in the membranes by cellulose/silica particles in PE. The permeability of carbondioxide, methane, oxygen, and nitrogen increased from 0.127, 0.008,0.034, and 0.007 barrer in pure polymer to 0.210, 0.012, 0.067and 0.017 barrer, respectively, in PE/cellulose/silica nanocomposite membranes containing 12wt% silica nanoparticles. In general, the permeability of gases increases by the following order:

$$P_{CH4}\,(38\%) < P_{N2}\,(58\%) < P_{CO2}\,(88\%) < P_{O2}\,(98\%)$$

As observed in the FE-SEM and TEM image, the presence of silica particles results in two groups of particles. The first group consists of micro-size particles which have a weak interaction with the polymer matrix and their contacting surface with the polymer matrix is also weak;it creates a free space at the intersection of particles and polymer. The second group includes the nanoparticles with a good interaction with the polymer matrix and good bonds with the polymer chains.The free space created in the intersection between polymer and microsilica can provide the space needed for the movement of gas molecules in polymer matrix, and it provides more opportunities for transportation of gas molecules through the membrane. Therefore, the permeability increases by silica content of PE/cellulose/silica membranes. Considerable increase in the permeability of carbon dioxide incomparison to other gases is related to structural changes occurring in the membranes. Such changes result from the presence of silica nanoparticles in the polymer matrix, leading to changes in the diffusion and solubility coefficient of gases in the polymer matrix. In the following, the reasons for such changes are investigated, stating the diffusion and solubility coefficients. Moreover, the increase in the free space enclosed by the polymer provides more suitable space for smaller gases to pass resulting in more increase in the permeability of smaller molecules.As shown in Figs4 and 5, the prepared membranes have dense structure with distributed nanospaces in the polymer particle interfaces.As a result, gas separation occurs based on solution-diffusion mechanism.

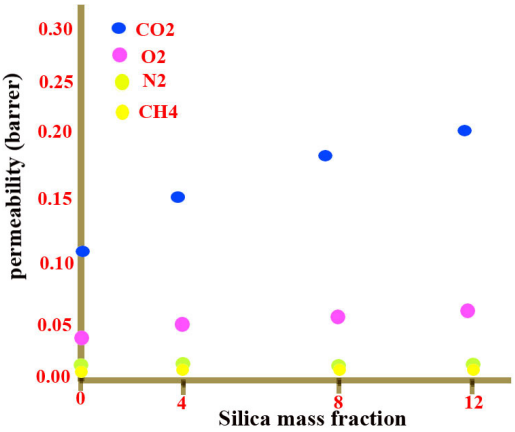

Fig. 9. Gas permeability of membranes at 25°C and the feed pressure of 10 barg

Fig. 10 shows the increment in selectivity of studied gases in nanocomposite membranes by silica. The selectivity of CO_2/N_2, CO_2/CH_4 and O_2/N_2 increases from 18.14, 15.87 and 4.16 to 19.11, 17.25 and 6.09 respectively, in nanocomposite membranes containing 12 wt% cellulose/silica nanocomposite. As reported in the FE-SEM and TEM analysis, addition of cellulose/silica nanocomposites in polymer creates some free spaces at the polymer-agglomerated particles. These free spaces would enhance the diffusion and solution of gases in polymer. As reported in Table 2, by addition of cellulose/silica nanoparticles to polymer the solubility selectivity of pair gases changes more than

Table 2. The solubility and diffusion selectivity for different gases at 25°C and the feed pressure of 10 barg

Solubility selectivity			Diffusivity selectivity			Membrane
S_{CO2}/S_{CH4}	S_{CO2}/S_{N2}	S_{O2}/S_{N2}	D_{CO2}/D_{CH4}	D_{CO2}/D_{N2}	D_{O2}/D_{N2}	
8.95	18.33	2.25	2.86	2.56	3.15	Pure PE
9.23	20.43	2.16	2.75	2.35	3.67	PE/cellulose/silica (4%)
8.77	21.65	2.13	2.77	2.21	3.71	PE/cellulose/silica (8%)
10.22	23.87	2.15	2.66	2.25	3.72	PE/cellulose/silica (12%)

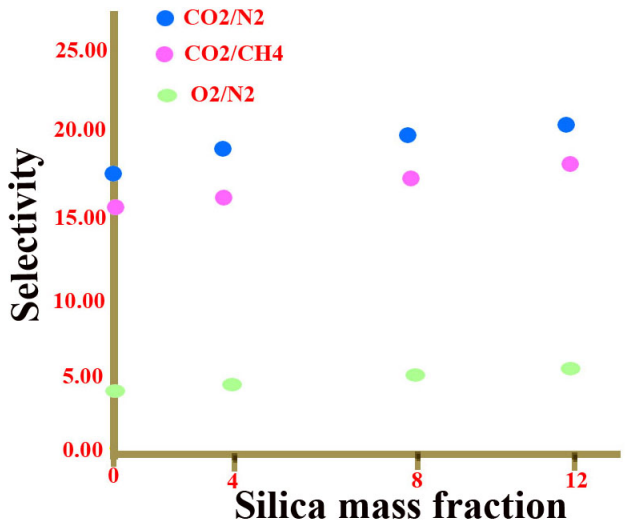

Fig. 10. CO_2/N_2, CO_2/CH_4 and O_2/N_2 ideal selectivity's of prepared nanocomposite membranes

diffusivity selectivity. It is due to spaces created in the polymer-agglomerated silica interface which enhance the higher sorption of small gases in comparison to others and finally lead to higher gas selectivity in polymer. Also, the results in Fig. 10 indicate the higher increment in the selectivity of CO_2/N_2 and CO_2/CH_4 pair gases compared to that of O_2/N_2. It is because of the increase in the solubility selectivity of carbon dioxide compared to nitrogen and methane, which will be discussed in the section dealing with the solubility coefficients. To evaluate the effect of silica nanoparticles in enhancing gas separation properties of PE/cellulose/silica membranes.

Effect of adding cellulose/silica nanoparticles on diffusion and solubility coefficients of gases

Table 2 shows the diffusion coefficient of different gases in the nanocomposite membranes. Fig. 11 indicates that the diffusion coefficients of all gases increase by the silica in the nanocomposite membranes. Also, it is clear that the changes in the diffusion coefficient of gases in pure polymer and nanocomposite membranes are as follows:

$$D_{CH4}<D_{N2}<D_{CO2}<D_{O2}$$

As it is obvious, the diffusion into the polymer is characterized by the molecular size, which is in turn determined by the kinetic diameter. The kinetic diameter is calculated only by the minimum diameter of the molecule profile and only indicates the minimum diameter needed for molecule to penetrate without considering the length of penetrating molecule. So, the diameter establishes a suitable relation with the penetration rate of the short molecules such as gas molecules including oxygen, nitrogen, and methane. Based on the diffusion theory, a gas molecule can penetrate when Brownian movement of the polymer chains provides enough space. This required space depends on the minimum cross-section and the length of penetrating molecule. This can serve as a reason for the linear relation between log D and the kinetic diameter of gas molecules, shown in Fig. 11 for pure PE and PE/cellulose/silica nanocomposite membranes. As shown in Fig.

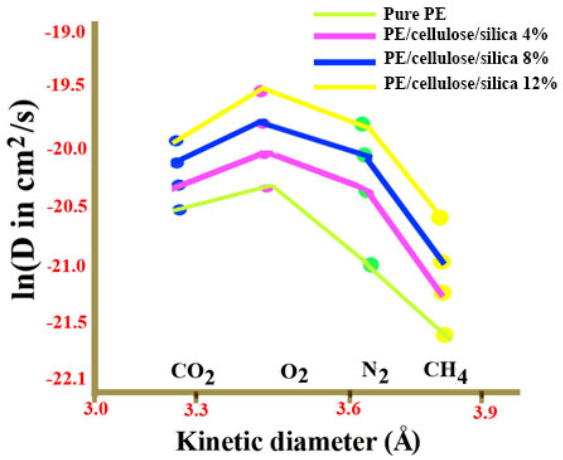

Fig.11. Correlation of diffusion coefficients to kinetic diameter of gases in composite membranes

11, carbon dioxide does not behave like other gases, and unlike what is expected for oxygen, its permeability does not decrease with the reduction in the kinetic diameter. This can be because of the carbon dioxide molecule is non-spherical and it has the double bond in its structure that prevents it from penetrating through the membrane(TabeMohammadi, *et al.*, 1995).

Solubility Coefficients

As it is clear, the gas sorption in polymeric membranes depends on the condensability of gases, interaction between the polymer and gas molecules, the structure of the polymer, temperature and pressure. The presence of an electron cloud on the double bond of carbon dioxide results in the increase in the instant bipolarity, and consequently better interaction of this molecule with polymer bonds. In addition to the above-mentioned reasons, it is easier for carbon dioxide to enter the free volumes in the polymer structure because of its smaller molecular size.

Table 2 shows the changes in the solubility coefficient of various gases in nanocomposite membranes. Considering above and the results given in Table 2, the order for solubility coefficient in the investigated membranes is as follows:

$$S_{CO2}>S_{CH4}>S_{O2}>S_{N2}$$

According to the obtained results, the solubility of gases increases based on their condensability. The presence of cellulose/silica particles results in the increase in the density of polar groups of OH in the polymer matrix, and consequently in the establishment of the polar spaces at the intersection of the particles and the polymer. Polar spaces result in an increase in the solubility coefficient of condensable gases. The solubility coefficient of carbon dioxide increases more than that of methane because of its polarity, and as a result, the possibility of formation of polar bonds with the polar groups. Table 2 shows the solubility and diffusion selectivity for different gases at 25°C and the feed pressure of 10 barg. Considering Table 2, after adding cellulose/silica nanoparticles, the solubility selectivity as well as its effect on the ideal selectivity will increase because of the increase in the solubility coefficient of carbon dioxide.

Antimicrobial Activity of PE/cellulose/silica nanocomposite membranes

Fig.12 shows the population growth of bacteria with increasing concentration of cellulose/silica nanoparticles to inhibit the Bacillus's cereus and E. coli growth which was confirmed by measuring turbidity. The purpose of plate counting is to estimate the number of cells present based on their ability to give rise to colonies under specific conditions of agar medium, temperature, and time. Both images in Fig.12 show that the number of viable colony decreases from the sample of cellulose/silica nanoparticles, as compared. For testing the cellulose/silica nanoparticles susceptibilities of B. cereus and E. coli, we used disc diffusion assay test. As it is evident from the results, cells were highly sensitive to all tested concentration of cellulose/silica nanoparticles, which was also confirmed from the size of the zone of inhibition. According to several research studies, it is accepted that the metal oxides carry the positive charge and the microorganism contains negative charge, due to the electromagnetic attraction between the microorganism and metal nanooxides. This leads to oxidization and in ally death of the microorganism. The cellulose/silica nanoparticles have been found to be a potent bactericidal compound, although compared to the established antibac-

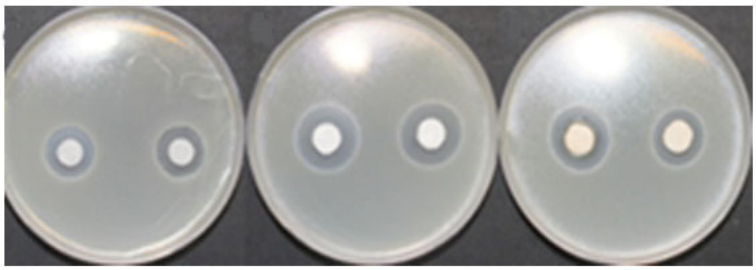

Fig. 12. Antimicrobial activity of s-PBI/cellulose/silica hybrid nanocomposites with (a) B. cereus (+) and (b) E. coli (−) for 24 h incubation at 37°C

terial compound such as ampicillin, but can be studied for superficial application as well as for combinational therapies. The inhibition growth of E. coli in the presence and absence of cellulose/silica nanoparticles has been done, which shows effect of subinhibitory and inhibitory concentration of cellulose/silica nanoparticle against the both B. cereus and E. coli till 24 h of incubation. The antimicrobial effect is greater than 5mm and E. coli for 8mm incubation studies. Therefore, the compression effect of both bacteria is greater for E. coli than for the B. cereus (Nabeshi, *et al.*, 2011, Agata, *et al.*, 1994).

CONCLUSIONS

In this present study is focused on synthesis of optically active bionanocomposite membranes. Cellulose/silica is used for enhancing strength and thermal resistance of PE membranes. It also exhibits good affinity for some gas molecules and can be used as potential silica in nanocomposite gas separation membrane preparation. The introduction of the bonding agent results in the reinforcing interfacial interaction between PE chains and the silica nanoparticles.The permeability of gases increases because of the creation of free spaces at the interface of the PE/cellulose/silica in the structure of PE. In general, the increase in the permeability of the gases was as follows:

$$P_{CH4}\ (38\%) < P_{N2}\ (58\%) < P_{CO2}\ (88\%) < P_{O2}\ (98\%)$$

Adding silica nanoparticles into the PE matrix, improved the separation performance of carbon dioxide/methane and carbon dioxide/nitrogen gases. The highest selectivity for carbon dioxide/nitrogen was 19.11 in the membranes containing 12 wt% of silica, and the highest selectivity for carbon dioxide/methane and for oxygen/nitrogen were 17.5 and 6.09, respectively, in the membranes containing 12 wt% of cellulose/silica. The diffusion coefficient for all gases, except for carbon dioxide, in all the membranes was proportional to the kinetic diameter. To determine the solubility coefficients of gases, the permeability coefficients were divided by the diffusion coefficients. The order of the solubility coefficients of gases in the studied membranes indicating that solubility of gases was increasing based on their condensability. Antimicrobial test against pathogenic bacteria was carried out. Therefore, the PE/cellulose/silica hybrid materials may find wide applications such as optoelectronics, sensor, biosensor, and also medical applications.

ACKNOWLEDGEMENTS

H. A. acknowledges financial support from Iran Nanotechnology Initiative Council (INIC).

REFERENCES

Albertson, A.C., Ljungquist, O., (1998). Degradable polyesters as biomaterials.ActaPolym, 39: 95-104.

Tudorachi, N.,Cascaval, C.N.,Rusu, M.,(2000). Biodegradable polymer blends based on polyethylene and natural polymers: Degradation in soil. J.Polym. Eng., 20 (4): 287-304.

Klemm, D., Heublein, B., Fink, H.P., Bohn, A.,(2005). Cellulose: Fascinating Biopolymer and Sustainable Raw Material. Angew Chem. Int. Ed Engl., 44 (22), 3358-3393.

Zimmerman, T., Pohler, E.,Schwaller, P.,(2005).Mechanical and Morphological Properties of Cellulose Fibril Reinforced Nanocomposites. Adv. Eng. Mater., 12: 1156-1161.

Habibi, Y., Lucia, L.A., Rojas, O.J., (2010). Cellulose Nanocrystals: Chemistry, Self-Assembly, and Applications. Chem. Rev., 110: 3479-3500.

Cao, X.D., Habibi, Y., Magalhaes, W.L.E., Rojas, O.J., Lucia, L.A.,(2011). Cellulose Nanocrystals-Based Nano composites: Fruits of a Novel Biomass Research and Teaching Platform. Curr. Sci., 100: 1172-1176.

Siro, I.,Plackett, D.,(2010).Microfibrillated Cellulose and New Nanocomposite Materials: A Review. Cellulose, 17: 459-494.

Liang, S.M., Zhang, L.N., Li, Y.F., Xu, J.,(2007). Fabrication and Properties of Cellulose Hydrated Membrane with Unique Structure. Macromol. Chem. and Phys., 208: 594-602.

Wu, Y.T., Zhou, Z., Fan, Q.Q., Chen, L., Zhu,

M.F.,(2009). Facile In-Situ Fabrication of Novel Organic Nanoparticle Hydrogels with Excellent Mechanical Properties. J. Mater. Chem., 19: 7340-7346.

Zheng, G., Cui, Y., Karabulut, E., Wagberg, L., Zhu, H., Hu, L., (2013). Nanostructured paper for lexible energy and electronic devices. MRS Bull., 38: 320-325.

Moon,R.J., Martini,A., Nairn,J., Simonsen,J.,Young blood, J., (2011).Cellulose nanomaterials review: structure, properties and nanocomposites. Chem. Soc. Rev., 40: 3941-3994.

Tobjork,D.,Osterbacka, R., (2011). Paper electronics. Adv.Mater., 23: 1935-1961.

Nyholm, L., Nystrom,G., Mihranyan,A.,Strømme, M., (2011).Toward lexible polymer and paper-based energy storage devices.Adv. Mater., 23: 3751-3769.

Song, G., Wang, L., Liu, D., Yao,J., Cao. Y., (2017). Gas transport properties of polyimide membranes bearing phenyl pendant group. High Perform Polym.,DOI: 10.1177/0954008316685411.

Athawale,V.D.,Lele,V., (1998). Graftcopolymerizationtostarch. II. Grafting of acrylic acid and preparation of its hydrogels.Carbohydr.Polym.,35: 21-27.

Chang, Y.T., Shu, C.F., Leu, C.M. and Wei, K.H., (2003). Synthesis and characterization of hyperbranched aromatic poly(ether imide)s with terminal amino groups. J.Polym.Sci. A, 41 (23): 3726-3736.

Hou, A., Wang, X., Wu, L., (2008). Effect of microwave irradiation on the physical properties and morphological structures of cotton cellulose.Carbohydr.Polym.,74: 934-937.

Innocenzi, P.,Lebeau, B., (2005). Organic-inorganic hybrid materials for non-linear optics.J. Mater. Chem., 15: 3821-3831.

Laine, R.M., Choi, J., Lee, I., (2001). Organic-inorganic nanocomposites with completely deined interfacial interactions. Adv. Mater., 13 (11): 800-803.

Von Nussbaum, F., Brands, M., Hinzen, B., Weigand, S.,Habich, D., (2006). Antibacterial natural products in medicinal chemistry-exodus or revival?Angew Chem. Int. Ed. Engl.45 (31): 5072-5129.

Tamaki, R., Tanaka, Y., Asuncion, M.Z., Choi, J., Laine, R.M., (2001).Octa(aminophenyl)silsesquioxane as a nanoconstruction site. J. Am. Chem. Soc., 123 (49): 12416-12417.

Tyan, H.L., Liu, Y.C., Wei, K.H., (1999). Thermally and mechanically enhance clay/polyimide nanocomposite via reactive organoclay. Chem. Mater., 11:1942-1947.

Abdalla, M.O., Dean, D., Campbell, S., (2002).Viscoelastic and mechanical properties of thermoset PMR-type polyimide-clay nanocomposites. Polymer, 43 (22): 5887-5893.

Zhang, J., Zhu, B.K., Chu, H.J., Xu, Y.Y., (2005). Silica/polyimide hybrids and their dielectric properties. I. Preparation with an improved sol-gel process with poly(amic acid) as the precursor. J. Appl. Polym. Sci., 97 (1): 20-24.

Ahmad, Z., Mark, J.E., (2001). Polyimide-ceramic hybrid composites by the sol-gel route. Chem. Mater., 13 (10): 3320-3330.

Dinari, M., Ahmadizadegan, H.,(2015).Novel and processable polyimides with a N-benzonitrile side chain: thermal, mechanical and gas separation properties. RSC Adv., 5: 26040-26050.

Ahmadizadegan,H., (2016). Synthesis and gas transport properties of novel functional polyimide/ZnO nanocomposite thin film membranes. RSC Adv. 6: 106778-106789.

Yu, Y. Liu, S., Wang, Y., Zhang, H., Li, X., Jiang Z., Liu,B., (2014). Asymmetric membranes prepared with trifluoromethylphenylatedpoly(ether ketone) for gas separation. High Perform Polym.,27 (1): 10-18.

Wu, C.Y., Hu, C.C., Lin, L.K., Lai, J.Y., Liu, Y.L.,(2016). Liberation of small molecules in polyimide membrane formation: An effect on gas separation properties. J. Membr. Sci., 499: 20-27.

Kim, J.H., Lee, Y.M., (2001). Gas permeation properties of poly(amide-6 b-ethylene oxide)- silica hybrid membranes. J.Membr. Sci., 193 (2): 209-225.

Ahmadizadegan H., (2017). Surface modification of TiO_2 nanoparticles with biodegradable nanocellolose and synthesis of novel polyimide/cellulose/TiO_2 membrane. Journal of Colloid and Interface Science, 491: 390-400.

Panndey, P., (2001). Chauhan RS Membranes for gas separation. Prog.Polym. Sci., 26: 853-893.

Sadeghi, M., Semsarzadeh, M.A., Moadel, H.,(2009). Enhancement of the gas separation properties of polybenzimidazole (PBI) membrane by incorporation of silica nano particles. J Membr Sci., 331: 21-30.

Qian, D., Dickey, E.C., Andrews, R., Rantell, T., (2000).Load transfer and deformation mechanisms in carbon nanotube-polystyrene composites. Appl. Phys. Lett., 76: 2868-2870.

Ahmadizadegan, H., (2016). Synthesis and Gas Transport Properties of Novel Functional Polyimide/ ZnO Nanocomposite Thin Film Membranes RSC Adv., 6: 106778-106789.

TabeMohammadi, A., Matsuura, T., Sourirajan, S.,(1995).Design and construction of gas permeation system for the measurement of low permeation rates and permeate compositions. J.Membr. Sci., 98: 281-286.

Nabeshi, H., Yoshikawa, T., Matsuyama, K., (2011). Systemic distribution, nuclear entry and cytotoxicity of amorphous nanosilica following topical application. Biomaterials, 32 (11): 2713-2724.

Agata, N., Mori, M., Ohta, M., Suwan, S., Ohtani, I., Isobe, M., (1994).A novel dodecadepsipeptide, cereulide, isolated from Bacillus cereus causes vacuole formation in HEp-2 cells.FEMS Microbiol. Lett., 121 (1): 31-34.

AUTHOR (S) BIOSKETCHES

Hashem Ahmadizadegan, Associate Professor,Department of Chemistry, Islamic Azad University, Darab Branch, Darab, Iran, *Email: h.ahmadizadegan.2005@gmail.com*

Mahdi Ranjbar, PhD, Department of Chemistry, Islamic Azad University, Darab Branch, Darab, Iran